
A Bayesian Solution To The Imitation Gap

Risto Vuorio*
University of Oxford
risto.vuorio@cs.ox.ac.uk

Mattie Fellows*
University of Oxford

Cong Lu*†
University of British Columbia
Vector Institute

Clémence Grislain
Sorbonne University ‡

Shimon Whiteson
University of Oxford

Abstract

In many real-world settings, an agent must learn to act in environments where no reward signal can be specified, but a set of expert demonstrations is available. Imitation learning (IL) is a popular framework for learning policies from such demonstrations. However, in some cases, differences in observability between the expert and the agent can give rise to an *imitation gap* such that the expert’s policy is not optimal for the agent and a naive application of IL can fail catastrophically. In particular, if the expert observes the Markov state and the agent does not, then the expert will not demonstrate the information-gathering behavior needed by the agent but not the expert. In this paper, we propose a Bayesian solution to the Imitation Gap (BIG), first using the expert demonstrations, together with a prior specifying the cost of exploratory behavior that is not demonstrated, to infer a posterior over rewards with Bayesian inverse reinforcement learning (IRL). BIG then uses the reward posterior to learn a Bayes-optimal policy. Our experiments show that BIG, unlike IL, allows the agent to explore at test time when presented with an imitation gap, whilst still learning to behave optimally using expert demonstrations when no such gap exists.

1 Introduction

Imitation learning [16, 27] is a powerful method for training policies when expert demonstration data is available for the desired behavior, without the need for explicit reward. However, standard imitation learning algorithms can fail when the expert demonstrator has access to privileged information that the imitator lacks. Specifically, if the expert observes the full Markov state, but the imitator operates under partial observability, then imitating expert behavior can lead to suboptimal performance [6, 7, 35]. This mismatch in observability is called the *imitation gap*.

For example, consider training a fruit-picking robot by learning from human demonstrations. Humans use a combination of visual cues and touch to quickly determine the ripeness of the fruit. They may reach out for a fruit that looks ripe, but then leave it on the branch to ripen more if it feels too hard in their hand. However, the robot has to rely on the visual cues alone since it lacks the sense of touch. If it then picks all fruit that look ripe on one side, it may end up picking many underripe fruit. A more intelligent robot would turn around fruit that looks borderline ripe to visually inspect them from all sides without detaching them from the branch. This exploratory behavior is never demonstrated, leading to an imitation gap, and hence naïvely imitating expert demonstrations leads to suboptimal behavior.

*Equal contribution

†Work done while at University of Oxford

‡Work done while interning at University of Oxford

At first glance, this problem seems intractable, since we cannot imitate behavior that is not demonstrated. Indeed, many prior solutions to the imitation gap often require privileged access to online reward information. The key insight in this paper is that the remaining uncertainty may be characterized in the form of a prior, specified over the cost of exploration in unobserved states. This leads us to propose a fully Bayesian solution to the Imitation Gap (BIG) which learns to behave Bayes-optimally at test-time, although its value will naturally be a function of the agent’s uncertainty.

We demonstrate how the prior can integrate several sources of information available before test time: we specify an initial reward prior, from which we may infer a posterior given a set of expert demonstrations and simulator, using Bayesian inverse reinforcement learning [26, BIRL] with successor features [3, 5, 12]. We also specify a reward prior over key exploration states to specify uncertainty about the *cost of exploration* where there is an imitation gap. This allows BIG to optimally trade off any remaining uncertainty about the true environment state using a Bayes-optimal policy, with the predictive reward under these priors as the fixed belief over rewards at test time. When there is an imitation gap, the reward prior can influence the agent’s behavior instead, yielding policies that *balance exploration to reduce the uncertainty in the environment with exploitation of expert demonstrations*. When there is no imitation gap, the agent can directly imitate expert behavior.

We evaluate BIG across a number of standard imitation gap problems, and further show that it scales to environments with high-dimensional observations. In each case, we can recover suitable reward functions from *only expert demonstrations and the cost of exploration prior*.

2 Preliminaries

Reinforcement Learning. We model the environment as a Markov Decision Process [29, MDP], defined as a tuple $\mathcal{M} := \langle \mathcal{S}, \mathcal{A}, p(s_{t+1}|s_t, a_t), p(s_0), r(s_t, a_t), \gamma \rangle$, where \mathcal{S} and \mathcal{A} denote the state and action spaces respectively, $p(s_{t+1}|s_t, a_t)$ the transition dynamics, $r(s_t, a_t)$ the reward function, and $p(s_0)$ the initial state distribution. We denote a sampled reward r . The goal in reinforcement learning is to optimize a policy $\pi(a|s)$ that maximizes the expected return $\mathbb{E}_{\pi, p} [\sum_{t=0}^{\infty} \gamma^t r(s_t, a_t)]$.

Learning from Demonstrations. We assume access to a set of expert demonstrations $\mathcal{D}_{\text{Expert}} := \{\tau_i\}_{i=1}^{N_{\text{Expert}}}$ of state-action trajectories $\tau_i := \{s_0, a_0, s_1, a_1, \dots\}$. In inverse reinforcement learning (IRL), the objective is to use these demonstrations to learn the reward function that the expert maximizes. In typical IRL methods, such as maximum entropy IRL [36], the reward function is learned alongside a policy that optimizes that function in a bi-level optimization algorithm.

By contrast, imitation learning is a closely related approach that seeks to directly mimic expert behavior from the demonstrations. This can be expressed as matching the distribution of the state-action pairs generated by the imitator to that of the expert [13, 15], i.e., minimizing the divergence between the limiting distribution over state-action pairs $D(\rho^*(s, a) \parallel \rho_{\pi}(s, a))$ where ρ^* and ρ_{π} are the state-action marginal distributions of the expert and the imitator policies respectively.

Successor Features. Successor features [3, SFs] are a value function representation that decouples the dynamics of the environment from the reward. Suppose that the reward function of the environment could be computed linearly as $r(s, a) = \nu(s, a)^{\top} \omega$ where $\nu(s, a) \in \mathbb{R}^d$ are features and $\omega \in \mathbb{R}^d$ are weights. For any given policy, we may then factor the Q -function as $Q^{\pi}(s, a, \omega) = \Psi^{\pi}(s, a)^{\top} \omega$ where $\Psi^{\pi}(s, a) := \mathbb{E}_{\tau \sim p^{\pi}} [\sum_{t=0}^{\infty} \gamma^t \nu(s_t, a_t) | s_0 = s, a_0 = a]$ is the successor feature of (s, a) under π .

3 Problem Setting

We now formalize the imitation gap in terms of a contextual MDP (CMDP) where the demonstrator, but not the imitator, observes a hidden parameter $\theta \in \Theta$ that affects the environment dynamics. Whilst the imitation gap could also be formalized in terms of partial observability in the state, we choose the CMDP formulation to make explicit what is hidden from the imitator and assume the states are fully observable. Formally, we define a CMDP as:

$$\mathcal{M}(\theta) := \langle \mathcal{S}, \mathcal{A}, p(s_{t+1}|s_t, a_t, \theta), p(s_0), r(s_t, a_t), \gamma \rangle,$$

with an underlying distribution over contexts $p(\theta)$. The reward function is independent of θ as we assume all tasks in the CMDP have a common goal (for example, driving safely at a junction), but

differ in their state transition dynamics. We are interested in policies that optimize the contextual expected, discounted return $\mathbb{E}_{p_{\infty}^{\pi}(\theta)} [\sum_{t=0}^{\infty} \gamma^t r(s_t, a_t)]$ where $p_{\infty}^{\pi}(\theta)$ is the distribution over infinite-horizon trajectories associated with policy π and context θ .

At test time, we are interested in behaving optimally in a CMDP $\mathcal{M}(\theta_{\text{test}})$ allocated according to the prior $\theta_{\text{test}} \sim p(\theta)$. Like other successor feature-based approaches [3, 5, 12, 17] we make the following assumption about the reward parametrization:

Assumption 3.1. The underlying reward function is bounded and can be represented as a linear function with respect to a reward feature vector $\nu(s, a)$ that is known a priori such that $r(s, a; \omega^*) = \nu(s, a)^{\top} \omega^* \in [r_{\min}, r_{\max}]$. Furthermore, the reward function is shared across all CMDPs, i.e., independent of θ .

This assumption simplifies our analysis and enables the derivation of convex optimization procedures. We do not assume oracle access to perfect reward features. Instead, the features could be the result of an unsupervised learning step external to our algorithm. Crucially, the agent can observe states and choose actions according to a policy but does *not* observe rewards nor θ_{test} and does not know the true reward parametrization ω^* . Instead, the agent is given a dataset of N_{Expert} demonstrations $\mathcal{D}_{\text{Expert}} := \{\tau_i\}_{i=1}^{N_{\text{Expert}}}$ of state-action trajectories $\tau_i := \{s_0, a_0, s_1, a_1, \dots\}$ of length H_i in CMDPs sampled from $p(\theta)$, where each expert $\pi_{\text{Expert}}^*(\cdot, \theta_i)$ behaves optimally in its assigned CMDP, e.g., expert trajectories of a car turning at a junction in summer and winter. Furthermore, the agent has access to a simulator, where CMDPs are allocated according to the prior $p(\theta)$, and the agent can interact with the corresponding environment, observing a trajectory of state-action pairs. We denote the complete dataset of simulated trajectories as $\mathcal{D}_{\text{Simulator}} := \{\tau_i\}_{i=1}^{N_{\text{Simulator}}}$. The agent never directly observes rewards nor θ_i in either $\mathcal{D}_{\text{Expert}}$ or $\mathcal{D}_{\text{Simulator}}$.

At test time, the agent is assigned a CMDP according to $\theta_{\text{test}} \sim p(\theta)$ and interacts with $\mathcal{M}(\theta_{\text{test}})$, obtaining a history of state-actions: $h_t := \{s_0, a_0, \dots, a_{t-1}, s_t\}$ at time t and takes actions according to a history-conditioned policy: $s_t \sim \pi(h_t)$. The agent never observes the reward history.

3.1 The Tiger-Treasure Problem

We introduce a variant of the classic ‘‘Tiger-Treasure Problem’’ from Kaelbling et al. [18] to illustrate how naively applying imitation learning fails when there is an imitation gap. Consider the CMDP in Figure 1 indexed by $\theta \in \{1, 2\}$, representing which door the tiger is behind. The prior is $p(\theta = 1) = p(\theta = 2) = 0.5$. In both CMDPs, the agent starts in state S_0 and the set of actions available is $\mathcal{A} = \{o_1, o_2, \text{listen}\}$, where o_1 and o_2 open the corresponding door and ‘listen’ listens for a tiger. In any state $s \in \{S_0, T_1, T_2\}$, the agent transitions deterministically to state Tiger if $a = o_1$ and $\theta = 1$ or $a = o_2$ and $\theta = 2$, and conversely for the Gold state. The goal of the agent is to reach the treasure (labeled ‘Gold’) whilst avoiding the Tiger. The agent receives a reward $r(\text{Gold}, \cdot) = 10$ for finding the gold and $r(\text{Tiger}, \cdot) = -100$ for finding the tiger. After this, the agent transitions to terminal state S_T regardless of action taken.

The agent can also listen before any doors are opened, receiving a stochastic signal with success rate $p > 0.5$ correlated with the identity of the door with the tiger. Hearing the tiger in room i transitions the agent to state T_i . For $s \in \{S_0, T_1, T_2\}$ and $a = \text{listen}$, the agent transitions to state T_1 with probability p if $\theta = 1$ and T_2 with probability p if $\theta = 2$, otherwise it transitions to state T_2 with probability $1 - p$ if $\theta = 1$ and T_1 with probability $1 - p$ if $\theta = 2$. States T_1 and T_2 are not present in Kaelbling et al. [18]’s original problem, but are included here because reward is assumed independent of θ and hence partial observability about the MDP is encoded in the state. Entering a listening state incurs a small negative reward $r(T_1, \cdot) = r(T_2, \cdot) = -1$. All other rewards not specified are 0.

For ease of exposition, assume the listening success $p = 1$. The expert has privileged knowledge about the MDP, and always chooses to open the door with the gold behind it. Consequently, expert demonstrations never feature listening actions. At test time, there is an imitation gap, as the agent

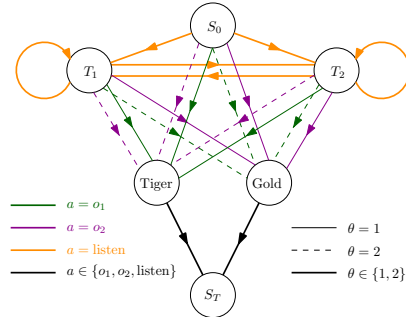


Figure 1: A diagram of the Tiger-Treasure Problem MDP, a classic example of an imitation gap. The agent initially does not know which door the treasure or tiger is behind and must take listening actions to resolve its uncertainty.

does not know a priori which door the tiger is behind. A naïve imitator does not realize that the expert is conditioning on extra information and so thinks the expert is randomly choosing which door to open; imitating that gives suboptimal return of -45γ . By contrast, an agent that chooses to listen always receives a return of $10\gamma - 1$ if it acts optimally on the revealed location of the tiger. This example demonstrates the failure of naïve imitation learning in simple settings when there is an imitation gap.

4 Towards a Bayesian Solution

In this paper, we propose a **Bayesian** solution to the **Imitation Gap** (BIG), where the goal is to learn a policy that can optimally trade-off its uncertainty at test time with imitating the expert demonstrator. Unlike in the canonical Bayesian RL setting, our formulation does not have access to reward samples from which to infer the underlying reward function. Instead, the reward prior determines the cost of exploration (COE) for the agent at test time, meaning that the agent can still behave optimally under partial observability. We provide an overall schematic of our approach in Figure 2.

BIG has three main phases which are labeled in Figure 2. In the first, we provide an initial prior over the reward parametrization $p(\omega)$. We integrate information from the expert data \mathcal{D}_{Exp} into the prior using a novel *contextual* Bayesian IRL (BIRL) approach (Sections 4.1 and 4.2) that infers the posterior $p(\omega|\mathcal{D}_{\text{Exp}})$. Because entire classes of reward functions can explain expert data equally well, IRL is an underspecified problem and approaches can equally penalize any unvisited state.

In the second phase (Section 4.3), we restrict the class of reward functions to those that allow for exploration at test time, by first normalizing the posterior so that the predictive reward lies in the range $[r_{\min}, r_{\max}]$ according to Assumption 3.1. Representing reward as $r = k \times r_{\max}$, we specify a cost of exploration prior $p(k)$ over rewards at key state-action pairs unseen in the expert demonstrations to integrate the cost of exploration information at test time. This approach ensures that all rewards still belong to the same *class* [25, Definition 1] after the IRL stage, i.e., yielding an equivalent optimal policy. This step is required as the expert demonstrations do not have full coverage. $p(k)$ encodes the relative cost of deviating from an optimal policy which encourages exploration for the downstream policy, complementing the IRL data. Integrating both the IRL and COE priors, we denote the Bayesian reward distribution as $p_{\text{Bayes}}^{\text{IRL+COE}}(r|s, a)$. We present pseudocode for an algorithm implementing the first and second phase in Appendix D.

In the third phase, we solve a Bayesian RL problem in which the goal is to learn a Bayes-optimal policy π_{Bayes} that can be deployed at test time. As shown in Figure 2, the inputs to the Bayes-adaptive MDP (BAMDP) are the Bayesian reward distribution $p_{\text{Bayes}}^{\text{IRL+COE}}(r|s, a)$ and a prior over context variables $p(\theta)$ (Section 4.4). The agent extracts reward information from the expert trajectories to learn a predictive reward but does not directly imitate the expert’s behavior and thus can adapt to the unknown MDP at test time, avoiding the problems with naïve imitation learning discussed in Section 3.1. Due to the diverse nature of the sources of input information, inferring the reward posterior requires the agent to learn and maintain several distributions over random variables, we summarize them in Table 1 in Appendix A.

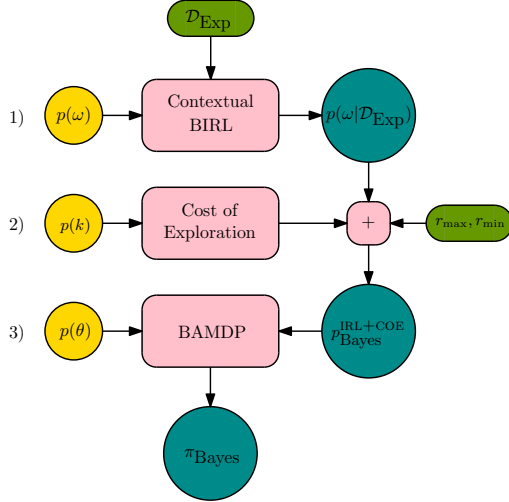


Figure 2: Schematic of the Bayesian solution to the Imitation Gap (BIG). Prior information is shown in green, algorithms in pink, prior distributions in yellow, and outputs in blue.

4.1 Contextual Successor Features

Before performing BIRL, we must learn a contextual value function representation to define the likelihood over expert trajectories. For an agent following policy π , we can characterize the expected discounted return as a function of state-action pairs via the contextual Q -function $Q^\pi(s, a, \theta, \omega)$, which satisfies the contextual Bellman equation: $\mathcal{B}^\pi[Q^\pi](s, a, \theta, \omega) = Q^\pi(s, a, \theta, \omega)$ where $\mathcal{B}^\pi[Q^\pi](s, a, \theta, \omega)$ is the contextual Bellman operator: $\mathcal{B}^\pi[Q^\pi](s, a, \theta, \omega) := \nu(s, a)^\top \omega + \gamma \mathbb{E}_{s' \sim p(s'|s, a, \theta), a' \sim \pi(a'|s')} [Q^\pi(s', a', \theta, \omega)]$.

Assumption 3.1 specifies a linear reward function, which allows us to use a *successor feature* representation of the Q -function that factors the reward parametrization out of $Q^\pi(s', a', \theta, \omega) = \Psi^\pi(s', a', \theta)^\top \omega$ where $\Psi^\pi(s, a, \theta)$ is the contextual successor feature, defined as: $\Psi^\pi(s, a, \theta) = \mathbb{E}_{\tau \sim p^\pi(\tau_\infty|\theta)} \left[\sum_{t=0}^{\infty} \gamma^t \nu(s_t, a_t) \middle| s_0 = s, a_0 = a \right]$. N.b., the reward is linear w.r.t. the features $\nu(s, a)$, which could themselves be learned and arbitrarily complex. Learning $\Psi^\pi(s, a, \theta)$ means that we do not need to solve a Bellman equation every time ω changes; we can simply take a dot product between the existing successor feature and the new ω . Appendix B details the training process.

4.2 Contextual Bayesian IRL

We now describe the first phase of our pipeline in Figure 2. Inferring the reward function is a Bayesian regression problem. As is typical for regression problems [22], we specify a Gaussian reward model $p(r|s, a, \omega) = \mathcal{N}(\nu(s, a)^\top \omega, I\sigma^2)$ with mean $\nu(s, a)$ and scalar variance parameter $\sigma \in \mathbb{R}$. We specify a Gaussian prior over the unknown reward parameterization $\mathcal{N}(\omega|\omega_0, I\sigma_0^2)$ where ω_0 is the prior mean and prior variance $\sigma_0^2 > 0$ represents the belief in ω_0 . Tuning σ_0^2 thus allows us to set how much the expert’s trajectories affect the prior reward specification after BIRL. We now exploit expert data to refine our prior by leveraging approaches from BIRL.

To derive the likelihood, it is necessary to define a model of the expert observations. In the classic Bayesian IRL approach [26], a likelihood is specified for a single MDP: $p(\tau_i|\omega)$. To adapt our approach to experts that act in multiple MDPs, our likelihood should account for the context $p(\tau_i|\theta_i, \omega) = \prod_{j=0}^{T_i-1} p(s_j, a_j|\theta_i, \omega)$. We assume that the agent’s policy is represented by a potential function defined by the optimal Q -function for the agent’s MDP:

$$p(a|s, \theta_i, \omega) = \frac{1}{z(s, \omega, \theta_i)} \exp\left(\frac{1}{\alpha} \Psi(s, a, \theta_i)^\top \omega\right),$$

where $z(s, \omega, \theta)$ is the normalization constant. Here α is a temperature parameter that controls how optimal the expert’s actions are with respect to $Q^*(s, a, \theta_i, \omega) = \Psi^*(s, a, \theta_i)^\top \omega$. As is convention [2, 26], this assumption stabilizes inference algorithms by softening the Dirac delta policy that the agent is following, allowing for gradients to flow into the density. A deterministic optimal policy is recovered in the limit $\alpha \rightarrow 0$.

Given the likelihood and prior, we infer the expert reward posterior $p(\omega|\mathcal{D}_{\text{Expert}})$. Marginalizing, we obtain the Bayesian reward distribution:

$$p_{\text{Bayes}}^{\text{IRL}}(r|s, a) := \mathbb{E}_{\omega \sim p(\omega|\mathcal{D}_{\text{Expert}})} [p(r|s, a, \omega)],$$

which incorporates both the epistemic uncertainty from the posterior and the aleatoric uncertainty from the reward model. Analogously to Bayesian logistic regression [22], using the potential function from Section 4.2 does not yield a closed-form solution for the posterior. Instead, we use the Laplace approximation for the posterior:

Theorem 4.1. Define $\zeta_0^2 := \frac{\sigma_0^2}{\alpha}$. Using the Laplace approximation, the approximate posterior is $p(\omega|\mathcal{D}_{\text{Expert}}) \approx \mathcal{N}(\omega|\omega_{\text{Laplace}}^*, \Sigma_{\text{Laplace}})$ where $\Sigma_{\text{Laplace}} = \nabla_\omega^2 \log p(\omega_{\text{Laplace}}^*|\mathcal{D}_{\text{Expert}})$ and $\omega_{\text{Laplace}}^*$ is the MAP estimate, which can be found by carrying out the following stochastic gradient descent updates on the log-posterior:

$$\omega \leftarrow \omega + \eta_\omega \left(N_{\text{Expert}} H_i \left(\Psi^*(s_j, a_j, \theta_i) - \mathbb{E}_{a_i \sim p(a_i|s_j, \omega, \theta_i)} [\Psi^*(s_j, a_i, \theta_i)] \right) - \frac{(\omega - \omega_0)}{\zeta_0^2} \right).$$

Proof. See Appendix F. □

The Bernstein von-Mises theorem formally justifies the approximation [8, 32], proving that under mild regularity assumptions, the posterior tends to the Laplace approximation in the limit of increasing data. ζ_0^2 controls how the prior influences learning; as $\zeta_0^2 \rightarrow 0$, expert data is ignored and $\omega_{\text{Laplace}}^* = \omega_0$. The posteriors over each expert’s contextual variable $p(\theta_i|\omega, \tau_i)$ typically have no closed-form analytic solution. We can approximate each $p(\theta_i|\omega, \tau_i)$ using variational inference instead, as detailed in Appendix E.

Role of Temperature. As IRL is underspecified, many reward functions can explain the expert data. A key insight from Theorem 4.1 is the role of the temperature parameter α in determining the relative difference between the lowest and highest rewards assigned. The example in Appendix G illustrates that when $\alpha \rightarrow 0$, the expert policy model becomes more deterministic, always choosing the action with the highest return. Arbitrarily small differences between rewards explain expert behavior, so IRL pulls the parametrization difference to be as small as possible. Conversely, when $\alpha \rightarrow \infty$, the expert policy becomes more stochastic, taking low-return actions more frequently in proportion to their value. An increasingly large separation in rewards is needed to explain expert behavior.

4.3 Cost of Exploration Prior

For the second phase, we specify a prior over the reward to incorporate information on the cost of exploration into the posterior reward returned by the contextual BIRL to refine the solution. Note that the imitation gap problem would not be solvable without access to prior information defining the cost of exploration, as the expert data does not demonstrate which states are safe to explore and how to balance exploration and exploitation. This prior is only introduced for exploration and does not need to contain any information about the exploitation, as that is learned from the expert demonstrations. Furthermore, the prior could be arbitrarily uninformative, in the third phase, our method learns the Bayes-optimal policy for any prior.

As shown in Figure 2, we start by rescaling the posterior reward to be within the bounds $[r_{\min}, r_{\max}]$ according to Assumption 3.1. We denote the corresponding scaled reward parametrization as $\tilde{\omega}_{\text{Bayes}}^*$. Given the infinite horizon, any linear transformation applied to the reward function results in the same optimal policy.

We assume that we know a subset of state-action pairs denoted as $\mathcal{S}_{\text{COE}} \times \mathcal{A}_{\text{COE}}$ where exploration can be performed. We illustrate this for the Tiger-Treasure problem from Figure 1; as rewards only depend on the state in this problem, the set is $\mathcal{S}_{\text{COE}} = \{T_1, T_2\}$. We introduce a simple COE inside the rescaled IRL reward parameterized by $\tilde{\omega}_{\text{Bayes}}^*$ by specifying a reward function $p(r|s, a, k) = \mathcal{N}(r|kr_{\max}, \sigma^2)$ over $(s, a) \in \mathcal{S}_{\text{COE}} \times \mathcal{A}_{\text{COE}}$ for some $k \in [\frac{r_{\min}}{r_{\max}}, 1]$; this ensures the mean is contained in $[r_{\min}, r_{\max}]$. A scale k that varies across action-state pairs may also be specified if a more complex cost of exploration information needs to be modeled. In the simple Tiger-Treasure problem, we know from construction the set of states where exploration can be performed. In a practical setting with large state space, these states could be obtained by considering non-expert, but safe behaviors from other policies acting in the same environment. This could require density estimation for continuous state spaces. We leave development of task specific cost of exploration priors for future work and focus on demonstrating the general principles in this work.

The value of k determines how risk-averse the agent is at test time. For $k \approx 1$ the agent values exploratory state-actions in $\mathcal{S}_{\text{COE}} \times \mathcal{A}_{\text{COE}}$ nearly as much as the most rewarding state-actions learned from IRL. As such, the cost of exploration is low, and the agent explores until it is highly certain about avoiding low reward actions in the imitation gap, encouraging conservative behavior. Conversely, as $k \rightarrow \frac{r_{\min}}{r_{\max}}$ the agent becomes less risk-averse and recovers a purely behavioral cloning regime, taking actions that could lead to low reward as they have similar value to exploratory actions.

To incorporate epistemic uncertainty in k , we specify a prior $p(k)$ with support over $[\frac{r_{\min}}{r_{\max}}, 1]$. Marginalizing, we obtain the Bayesian reward distribution over $\mathcal{S}_{\text{COE}} \times \mathcal{A}_{\text{COE}}$:

$$p_{\text{Bayes}}^{\text{COE}}(r|s, a) = \mathbb{E}_{k \sim p(k)} [p(r|s, a, k)].$$

For all other state-action pairs, the Bayesian reward distribution remains unchanged, yielding the distribution over $\mathcal{S} \times \mathcal{A}$:

$$p_{\text{Bayes}}^{\text{IRL} + \text{COE}}(r|s, a) = \begin{cases} p_{\text{Bayes}}^{\text{COE}}(r|s, a) & s, a \in \mathcal{S}_{\text{COE}} \times \mathcal{A}_{\text{COE}}, \\ p_{\text{Bayes}}^{\text{IRL}}(r|s, a) & \text{otherwise.} \end{cases}$$

4.4 Bayes-Optimal Policy Learning

For the third phase, we perform Bayesian reinforcement learning, which optimally trades off exploration and exploitation by conditioning actions on the agent’s uncertainty over θ . We can define a Bayes-adaptive MDP [9, BAMDP] using the contextual MDP in Section 3 as a model. At test time, the agent is assigned an MDP $\theta_{\text{test}} \sim p(\theta_{\text{test}})$ and can observe samples from $p(s'|s, a, \theta_{\text{test}})$ by interacting with the MDP via its policy. A history of interactions is denoted $h_t := \{s_0, a_0, s_1, a_1, \dots, s_t\} \in \mathcal{H}_t$ where \mathcal{H}_t is the corresponding state-action product space. After observing a history h_t from the assigned MDP, the agent updates its belief in θ_{test} according to the posterior:

$$p(\theta_{\text{test}}|h_t) = \frac{\prod_{i=1}^t p(s_i|s_{i-1}, a_{i-1}, \theta_{\text{test}})p(\theta_{\text{test}})}{\mathbb{E}_{\theta_{\text{test}} \sim p(\theta_{\text{test}})} \left[\prod_{i=1}^t p(s_i|s_{i-1}, a_{i-1}, \theta_{\text{test}}) \right]}.$$

Using the posterior, we can define the Bayesian transition distribution as:

$$p(s_{t+1}|h_t, a_t) = \int_{\Theta} p(s_{t+1}|s_t, a_t, \theta_{\text{test}})p(\theta_{\text{test}}|h_t)d\theta_{\text{test}}.$$

As there is no reward signal available to the agent and rewards do not depend on θ , the Bayesian reward distribution in the BAMDP is exactly the combined Bayesian reward distribution from Section 4.3: $p(r_t|h_t, a_t) = p_{\text{Bayes}}^{\text{IRL} + \text{COE}}(r_t|s_t, a_t)$. We denote the joint reward-state Bayesian transition distribution as $p(r_t, s_{t+1}|s_t, a_t) = p(r_t|h_t, a_t)p(s_{t+1}|h_t, a_t)$, which is equivalent to the predictive trajectory transition distribution: $p(\tau_{t+1}|\tau_t, a_t) = p(\tau_t, a_t, r_t, s_{t+1}|\tau_t, a_t) = p(r_t, s_{t+1}|h_t, a_t) \underbrace{p(\tau_t, a_t|\tau_t, a_t)}_{=1} =$

$p(r_t, s_{t+1}|h_t, a_t)$. Here $p(\tau_{t+1}|\tau_t, a_t)$ is used to reason over unobserved counterfactual trajectories, and so must account for predictive reward. We define the corresponding BAMDP similarly to Fellows et al. [10] as $\mathcal{M}_{\text{BAMDP}} := \langle \mathcal{T}, \mathcal{A}, p(\tau_{t+1}|\tau_t, a_t), p(s_0), \gamma \rangle$ where \mathcal{T} is the space of all possible trajectories.

In Bayesian RL, policies $\pi_{\text{Bayes}}(a_t|h_t)$ map from *histories* to distributions over actions, and our goal is to learn a Bayes-optimal policy $\pi_{\text{Bayes}}^*(a_t|h_t)$ that solves $\mathcal{M}_{\text{BAMDP}}$. Due to the linearity of our formulation, we show in Appendix F.1 that solving the BAMDP is equivalent to optimizing the following Bayesian RL objective for π_{Bayes} :

$$J_{\text{Bayes}}^{\pi} = \mathbb{E}_{p(\theta_{\text{test}})} \left[\mathbb{E}_{p(h_{\infty}|\theta_{\text{test}})} \left[\sum_{i=0}^{\infty} \gamma^i r_{\text{Bayes}}^{\text{IRL} + \text{COE}}(s_i, a_i) \right] \right],$$

where $p(h_{\infty}|\theta_{\text{test}}) = p_0(s_0) \prod_{i=0}^{\infty} p(s_{i+1}|s_i, a_i, \theta_{\text{test}})\pi(a_i|h_i)$, and $r_{\text{Bayes}}^{\text{IRL} + \text{COE}}(s, a)$ is the predictive reward:

$$r_{\text{Bayes}}^{\text{IRL} + \text{COE}}(s, a) := \begin{cases} r_{\max} \mathbb{E}_{k \sim p(k)} [k] & s, a \in \mathcal{S}_{\text{COE}} \times \mathcal{A}_{\text{COE}}, \\ \nu^{\top}(s, a) \bar{\omega}_{\text{Bayes}}^* & \text{otherwise.} \end{cases}$$

In the following empirical evaluation, we approximate Bayes-optimal policies by training a policy conditioned on the true inference model using DQN [21].

5 Empirical Evaluation

To evaluate BIG, we conduct experiments across a series of imitation gap problems. In all the tested environments, the agent has to solve a task that requires exploration. First, we demonstrate that in the Tiger-Treasure environment, naive IRL learns a reward function that does not lead to the desired exploratory policy, whereas BIG does by exploiting prior information about the cost of exploration. Second, we illustrate that, by marginalizing over the context distribution, naive IRL can learn a reward function that does not capture the expert’s intent. Finally, we present results in a gridworld environment to show that BIG can handle imitation learning tasks with larger state-action spaces. Since we assume no access to true environment reward or expert state information, most previous solutions to the imitation gap are not applicable. Instead, we compare to maximum entropy IRL (labeled ‘No-Prior’ in our experiments). For convenience, we implement Algorithm 1 using the true posterior $p(\theta|\tau)$ as the inference model. In all experiments, we use deep neural networks for Ψ . We assume normally distributed errors and report standard error across seeds in the figures.

5.1 Investigating Reward Priors

In the Tiger-Treasure environment introduced in Section 3.1, since the expert always goes to the treasure room directly, we cannot extract information about optimal exploration from the expert data. As discussed in Section 4.3, we use the prior $p(k)$ to enable exploratory behavior at test time. We explore the influence of this reward prior on the environment from Figure 1, using a space of uniform priors $p(k) = \text{Unif}([a, b])$ over intervals $[a, b] \in \left[\frac{r_{\min}}{r_{\max}}, 1\right)$. We choose $r_{\min} = -100$ and $r_{\max} = 10$. While these bounds are arbitrary, they reflect the undesirability of failing in the task demonstrated by the expert. The reward feature ν is a one-hot indicator over the states. Figure 3 presents the agent’s success rate in reaching the treasure, along with the average time exploring, which corresponds to the number of listening actions, for different values of the prior mean k^* . As expected from Section 4.3, when k^* approaches 1, the agent explores more, never exploiting when $k^* = 1$. The probability of reaching the treasure increases with the number of listening actions. Therefore, as k^* approaches 1 (without reaching it), the treasure rate also increases. By contrast, when k^* decreases the agent begins to listen less often. These behaviors correspond to the Bayes-optimal policies for each of the priors, demonstrating that our method learns the Bayes-optimal policy irrespective of the prior supplied.

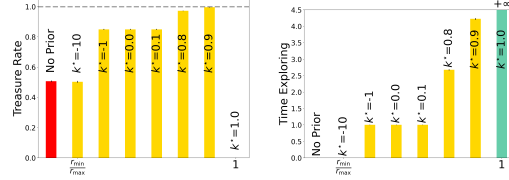


Figure 3: Evaluation of BIG in the Tiger-Treasure environment. Success rate and time exploring (in steps) for policies learned with a uniform prior reward with different means are represented in yellow ($k^* < 1$) and in green ($k^* = 1$), while the case with no prior is shown in red. Error bars indicate the standard error of the mean across 10 seeds. The symbol $+\infty$ indicates that, for some trials, the agent explores throughout the entire (infinite) episode.

5.2 Investigating Latent Inference

Next, we look at whether inferring the latent θ during IRL matters for learning the desired reward function. We experiment in a simple CMDP environment depicted in Figure 4. For a mathematical example, see Appendix C. In this environment, the expert policy goes to the state s_3 , which provides a reward of +2 and then loops back to state s_0 through s_4 or s_5 . It prefers to take the route through s_1 , when it is available, to avoid the negative reward of -1 in s_2 . When θ is distributed such that $p(\theta = 0) > p(\theta = 1)$, it can lead to naive IRL misidentifying the expert intent. To see why, consider that to fit the expert behavior without information about θ , the reward function has to make the path through s_2 more likely in both MDPs. Conditioning the successor features on the inferred θ resolves this issue, because then identifying the reward reduces to standard IRL in two separate MDPs. To verify this in practice, we show results of learning the reward functions with and without latent inference in Figure 4. We choose the latent to be distributed as $p(\theta = 0) = 0.9$. No reward prior is used. The policy trained on the rewards learned with latent inference matches the policy trained with the ground truth rewards. The rewards learned without latent inference do not result in as good a policy, demonstrating that latent inference is necessary to learn the correct rewards in a general CMDP. See Appendix H.2 for an analysis of the learned rewards.

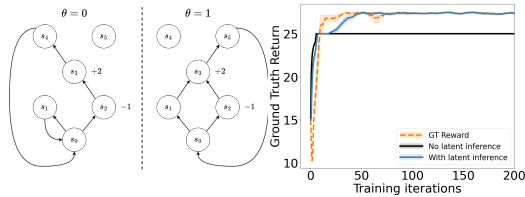


Figure 4: A demonstration of the necessity for latent inference with BIG. On the left, we show the CMDP used in the experiments, with two possibilities for the context θ . On the right, we show the ground truth returns of a DQN agent for trajectories of 100 steps in the CMDP during training. The shading shows the standard error of the mean for 8 seeds.

5.3 Reward Priors in a Larger CMDP

Finally, we test BIG in a grid-world environment with pixel-based observations. The agent observes a top-down view of the environment similar to the illustration of the learned rewards presented in Figure 5. The agent can move in four directions and take listening actions. Taking the listening action in any grid cell results in a stochastic transition to a state, which indicates the location of the gold, but otherwise has the same dynamics as the cell that the action was taken in. When the agent enters a door, it is moved to Tiger or Gold depending on θ . From those states, the agent is moved to the

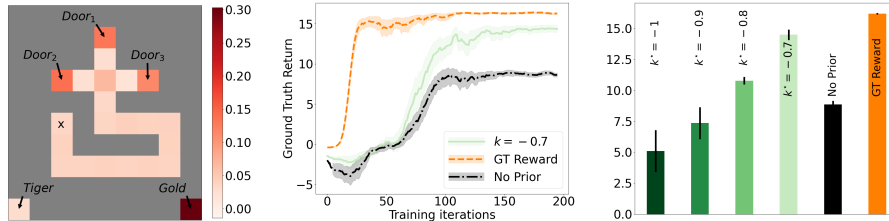


Figure 5: BIG successfully learns the optimal behavior in a challenging gridworld environment. On the left, we show the rewards learned by the contextual IRL. In the middle, we show the return (using the manually constructed reward) of policies trained with reward inferred with and without a reward prior and the manually constructed reward (ground truth). The shading shows the standard error of the mean for 8 random seeds. On the right, we show the final returns of policies trained using different values of k^* compared to not using the reward prior and using the ground truth reward.

grid cell marked with x in the next timestep, setting the agent up for another round in the maze. The expert takes the shortest path from any state to Gold, choosing the correct door, depending on θ . See Appendix H.4 for details.

Three DQN training curves are shown in Figure 5 corresponding to a manually constructed ground truth reward, which explains the expert behavior, reward learned by the contextual IRL without using a reward prior, and the same reward refined using the prior. These learning curves show that BIG with a particular reward prior produces a similar BAMDP policy as the manually constructed reward. At the same time, using just the IRL reward results in a policy that initially chooses a door at random. We compare multiple values for k^* and find that as in the simple Tiger-Treasure environment, different values result in over-exploration or under-exploration leaving a range in the middle that results in similar exploration as the handcrafted reward. This experiment shows that BIG can recover a reward function, which enables the agent to complete the task demonstrated by the expert despite a challenging imitation gap.

6 Related Work

Imitation Gaps. Prior work addressing the imitation gap typically assumes privileged access to the true environment reward during training. In contrast, BIG makes no such assumption. Nguyen et al. [23], Weihs et al. [35] assume access to the true reward during training, and propose to bridge the imitation gap by training on a weighted imitation and RL loss. Other works propose to also integrate privileged information about the expert during training [7] in addition to the reward. For example, Elf Distillation [34] studies an approach that mixes environment reward with online advice from the expert. Cai et al. [6] propose several stages of training, including those on privileged expert states, to connect the imitator and expert’s observation spaces. Separately, versions of the imitation gap have been considered by Kwon et al. [20], Ortega et al. [24], Swamy et al. [30], Vuorio et al. [33] that assume that no new exploratory behavior needs to be learned. The setting considered by Straub et al. [28] is closer to our work but it only considers inferring unknown parameters from an agent acting under partial observability (that is, the IRL problem). Our setting also requires an agent to act optimally in an *unknown* environment *without* a reward signal, i.e., there is uncertainty in the MDP at test time.

Bayesian Reinforcement Learning. Our work shares similar components to other Bayesian approaches to RL. For instance, VariBAD and related methods [37–39] consider a model-based approach for learning approximations to Bayes-optimal policies by exploiting meta-reinforcement learning [4] to perform inference over a subset of the unobserved context. Similarly, BEN [11] is a model-free approach that learns Bayes-optimal policies by specifying a model and prior over the optimal Bellman operator. All of these methods assume access to the reward and do not consider the issue of imitating an expert. Bayesian Inverse RL approaches infer a posterior over the unknown reward distribution given trajectories of demonstrations [26] (see Adams et al. [1], Table 1 for a complete list of existing approaches). BIG generalizes these approaches in Section 4.2 to account for the unobserved context variable before integrating the learned reward posterior into a BAMDP.

Successor Features. Successor features [3, 5] provide an elegant representation of value functions under the assumptions of a linear reward function. Janz et al. [17] incorporate successor features

into the Bayesian framework. Most similar to BIG, successor features have been used successfully in Psi-Phi Learning [12] for multi-task inverse reinforcement learning. Psi-Phi Learning can also retrieve the reward parameterizations for a new agent (expert) but does so with full observability.

7 Limitations

To make the empirical setup close to the theory, we use ground truth inference models and linearity assumptions, which means that scaling up the algorithm requires revisiting those choices. For example, by learning an approximate inference model. In the CMDPs considered in this paper, we assumed the set of allowed exploration states was explicitly known a priori, which may be a limiting assumption in harder problems. As is typical in Bayesian methods, we leave the design of problem-specific priors to the practitioners focused on those problems.

8 Conclusion

In this paper, we proposed a fully Bayesian solution to the imitation gap which integrated various priors over the reward parameterization, cost of exploration, and hidden state. This allowed us to derive a BAMDP formulation of the problem whose solution optimally trades off exploration and exploitation at test time. We demonstrated the importance of each component of our algorithm across a series of experiments with an imitation gap before showing that BIG scales to larger maze problems, including those with high-dimensional pixel-based observations. Crucially, in contrast to previous work, no online reward information was required. This makes our work particularly exciting for challenging imitation problems where no reward is easily specifiable, and extending BIG to even more complex settings is a promising direction for future work.

References

- [1] Stephen Adams, Tyler Cody, and Peter A. Beling. A survey of inverse reinforcement learning. *Artif. Intell. Rev.*, 55(6):4307–4346, aug 2022. ISSN 0269-2821. doi: 10.1007/s10462-021-10108-x. URL <https://doi.org/10.1007/s10462-021-10108-x>.
- [2] Saurabh Arora and Prashant Doshi. A survey of inverse reinforcement learning: Challenges, methods and progress. *Artificial Intelligence*, 297:103500, 2021. ISSN 0004-3702. doi: <https://doi.org/10.1016/j.artint.2021.103500>. URL <https://www.sciencedirect.com/science/article/pii/S0004370221000515>.
- [3] Andre Barreto, Will Dabney, Remi Munos, Jonathan J Hunt, Tom Schaul, Hado P van Hasselt, and David Silver. Successor features for transfer in reinforcement learning. In I. Guyon, U. Von Luxburg, S. Bengio, H. Wallach, R. Fergus, S. Vishwanathan, and R. Garnett, editors, *Advances in Neural Information Processing Systems*, volume 30. Curran Associates, Inc., 2017. URL https://proceedings.neurips.cc/paper_files/paper/2017/file/350db081a661525235354dd3e19b8c05-Paper.pdf.
- [4] Jacob Beck, Risto Vuorio, Evan Zheran Liu, Zheng Xiong, Luisa Zintgraf, Chelsea Finn, and Shimon Whiteson. A survey of meta-reinforcement learning. *arXiv preprint arXiv:2301.08028*, 2023.
- [5] Daniel S. Brown and Scott Niekum. Deep bayesian reward learning from preferences. *Workshop on Safety and Robustness in Decision Making. 33rd Conference on Neural Information Processing Systems (NeurIPS 2019)*, abs/1912.04472, 2019. URL <https://arxiv.org/pdf/1912.04472.pdf>.
- [6] Xin-Qiang Cai, Yao-Xiang Ding, Zi-Xuan Chen, Yuan Jiang, Masashi Sugiyama, and Zhi-Hua Zhou. Seeing differently, acting similarly: Heterogeneously observable imitation learning. *arXiv preprint arXiv:2106.09256*, 2021.
- [7] Dian Chen, Brady Zhou, Vladlen Koltun, and Philipp Krähenbühl. Learning by cheating. In *Conference on Robot Learning (CoRL)*, 2019.
- [8] J. L. Doob. Application of the theory of martingales. *Colloques Internationaux du Centre National de la Recherche Scientifique*, pages 23–27, 1949.
- [9] Michael O’Gordon Duff. *Optimal Learning: Computational procedures for Bayes-adaptive Markov decision processes*. University of Massachusetts Amherst, 2002.
- [10] Mattie Fellows, Brandon Kaplowitz, Christian Schroeder de Witt, and Shimon Whiteson. Bayesian exploration networks. *arXiv preprint arXiv:2308.13049*, 2023.
- [11] Mattie Fellows, Matthew J. A. Smith, and Shimon Whiteson. Why target networks stabilise temporal difference methods. In Andreas Krause, Emma Brunskill, Kyunghyun Cho, Barbara Engelhardt, Sivan Sabato, and Jonathan Scarlett, editors, *Proceedings of the 40th International Conference on Machine Learning*, volume 202 of *Proceedings of Machine Learning Research*, pages 9886–9909. PMLR, 23–29 Jul 2023. URL <https://proceedings.mlr.press/v202/fellows23a.html>.
- [12] Angelos Filos, Clare Lyle, Yarin Gal, Sergey Levine, Natasha Jaques, and Gregory Farquhar. Psiphi-learning: Reinforcement learning with demonstrations using successor features and inverse temporal difference learning, 2021.
- [13] Chelsea Finn, Sergey Levine, and Pieter Abbeel. Guided cost learning: Deep inverse optimal control via policy optimization. In *International conference on machine learning*, pages 49–58. PMLR, 2016.
- [14] Elad Hazan, Sham Kakade, Karan Singh, and Abby Van Soest. Provably efficient maximum entropy exploration. In Kamalika Chaudhuri and Ruslan Salakhutdinov, editors, *Proceedings of the 36th International Conference on Machine Learning*, volume 97 of *Proceedings of Machine Learning Research*, pages 2681–2691. PMLR, 09–15 Jun 2019. URL <https://proceedings.mlr.press/v97/hazan19a.html>.

- [15] Jonathan Ho and Stefano Ermon. Generative adversarial imitation learning. *Advances in neural information processing systems*, 29, 2016.
- [16] Ahmed Hussein, Mohamed Medhat Gaber, Eyad Elyan, and Chrisina Jayne. Imitation learning: A survey of learning methods. *ACM Computing Surveys (CSUR)*, 50(2):1–35, 2017.
- [17] David Janz, Jiri Hron, Przemysław Mazur, Katja Hofmann, José Miguel Hernández-Lobato, and Sebastian Tschiatschek. Successor uncertainties: Exploration and uncertainty in temporal difference learning. In *Proceedings of the 33rd International Conference on Neural Information Processing Systems*, Red Hook, NY, USA, 2019. Curran Associates Inc.
- [18] Leslie Pack Kaelbling, Michael L Littman, and Anthony R Cassandra. Planning and acting in partially observable stochastic domains. *Artificial intelligence*, 101(1-2):99–134, 1998.
- [19] Diederik P Kingma and Max Welling. Auto-encoding variational bayes. In *International Conference on Learning Representations*, 2014.
- [20] Minhae Kwon, Saurabh Daptardar, Paul R Schrater, and Xaq Pitkow. Inverse rational control with partially observable continuous nonlinear dynamics. *Advances in neural information processing systems*, 33:7898–7909, 2020.
- [21] Volodymyr Mnih, Koray Kavukcuoglu, David Silver, Alex Graves, Ioannis Antonoglou, Daan Wierstra, and Martin Riedmiller. Playing atari with deep reinforcement learning. *arXiv preprint arXiv:1312.5602*, 2013.
- [22] Kevin P. Murphy. *Machine learning : a probabilistic perspective*. MIT Press, Cambridge, Mass. [u.a.], 2013. ISBN 9780262018029 0262018020.
- [23] Hai Huu Nguyen, Andrea Baisero, Dian Wang, Christopher Amato, and Robert Platt. Leveraging fully observable policies for learning under partial observability. In *6th Annual Conference on Robot Learning*, 2022.
- [24] Pedro A Ortega, Markus Kunesch, Grégoire Delétang, Tim Genewein, Jordi Grau-Moya, Joel Veness, Jonas Buchli, Jonas Degraeve, Bilal Piot, Julien Perolat, Tom Everitt, Corentin Tallec, Emilio Parisotto, Tom Erez, Yutian Chen, Scott Reed, Marcus Hutter, Nando de Freitas, and Shane Legg. Shaking the foundations: delusions in sequence models for interaction and control. October 2021.
- [25] Rafael Rafailov, Archit Sharma, Eric Mitchell, Stefano Ermon, Christopher D. Manning, and Chelsea Finn. Direct preference optimization: Your language model is secretly a reward model. *NeurIPS*, abs/2305.18290, 2023. URL <https://api.semanticscholar.org/CorpusID:258959321>.
- [26] Deepak Ramachandran and Eyal Amir. Bayesian inverse reinforcement learning. In *Proceedings of the 20th International Joint Conference on Artificial Intelligence, IJCAI’07*, page 2586–2591, San Francisco, CA, USA, 2007. Morgan Kaufmann Publishers Inc.
- [27] Stefan Schaal. Is imitation learning the route to humanoid robots? *Trends in cognitive sciences*, 3(6):233–242, 1999.
- [28] Dominik Straub, Matthias Schultheis, Heinz Koepl, and Constantin A Rothkopf. Probabilistic inverse optimal control for non-linear partially observable systems disentangles perceptual uncertainty and behavioral costs. *Advances in Neural Information Processing Systems*, 36, 2024.
- [29] Richard S. Sutton and Andrew G. Barto. *Reinforcement Learning: An Introduction*. The MIT Press, second edition, 2018. URL <http://incompleteideas.net/book/the-book-2nd.html>.
- [30] Gokul Swamy, Sanjiban Choudhury, J Andrew Bagnell, and Zhiwei Steven Wu. Sequence model imitation learning with unobserved contexts. *Advances in Neural Information Processing Systems*, 35, 2022.

- [31] J.N. Tsitsiklis and B. Van Roy. An analysis of temporal-difference learning with function approximation. *IEEE Transactions on Automatic Control*, 42(5):674–690, 1997. doi: 10.1109/9.580874.
- [32] A.W. van der Vaart. *Asymptotic Statistics*. Cambridge series on statistical and probabilistic mathematics. Cambridge University Press, 1998. ISBN 9780521496032. URL <https://books.google.co.uk/books?id=fiX9ngEACAAJ>.
- [33] Risto Vuorio, Johann Brehmer, Hanno Ackermann, Daniel Dijkman, Taco Cohen, and Pim de Haan. Deconfounded imitation learning. *arXiv preprint arXiv:2211.02667*, 2022.
- [34] Aaron Walsman, Muru Zhang, Sanjiban Choudhury, Dieter Fox, and Ali Farhadi. Impossibly good experts and how to follow them. In *The Eleventh International Conference on Learning Representations*, 2023. URL https://openreview.net/forum?id=sciA_xgYofB.
- [35] Luca Weihs, Unnat Jain, Iou-Jen Liu, Jordi Salvador, Svetlana Lazebnik, Aniruddha Kembhavi, and Alex Schwing. Bridging the imitation gap by adaptive insubordination. In A. Beygelzimer, Y. Dauphin, P. Liang, and J. Wortman Vaughan, editors, *Advances in Neural Information Processing Systems*, 2021. URL https://openreview.net/forum?id=Wlx0DqiUTD_.
- [36] Brian D Ziebart, Andrew L Maas, J Andrew Bagnell, Anind K Dey, et al. Maximum entropy inverse reinforcement learning. In *Aaai*, volume 8, pages 1433–1438. Chicago, IL, USA, 2008.
- [37] Luisa Zintgraf, Kyriacos Shiarlis, Maximilian Igl, Sebastian Schulze, Yarin Gal, Katja Hofmann, and Shimon Whiteson. Varibad: A very good method for bayes-adaptive deep rl via meta-learning. In *International Conference on Learning Representations*, 2020.
- [38] Luisa Zintgraf, Sebastian Schulze, Cong Lu, Leo Feng, Maximilian Igl, Kyriacos Shiarlis, Yarin Gal, Katja Hofmann, and Shimon Whiteson. Varibad: Variational bayes-adaptive deep rl via meta-learning. *Journal of Machine Learning Research*, 22(289):1–39, 2021. URL <http://jmlr.org/papers/v22/21-0657.html>.
- [39] Luisa M Zintgraf, Leo Feng, Cong Lu, Maximilian Igl, Kristian Hartikainen, Katja Hofmann, and Shimon Whiteson. Exploration in approximate hyper-state space for meta reinforcement learning. In Marina Meila and Tong Zhang, editors, *Proceedings of the 38th International Conference on Machine Learning*, volume 139 of *Proceedings of Machine Learning Research*, pages 12991–13001. PMLR, 18–24 Jul 2021. URL <https://proceedings.mlr.press/v139/zintgraf21a.html>.

Supplementary Material

A Summary of Distributions in BIG

Due to the diverse nature of the sources of input information, inferring the reward posterior requires the agent to learn and maintain several distributions over random variables, we summarize them in Table 1.

Table 1: Summary of the distributions involved in BIG. This table supplements the diagram in Figure 2.

DISTRIBUTION	NAME	DESCRIPTION	SAMPLES TO LEARN
$p(\omega)$	Reward Parameter Prior	Incorporates prior knowledge in reward parameterization	None
$p(k)$	Cost of Exploration Prior	Incorporates prior knowledge in rewards $r(s, a) = kr_{\max}$ over exploratory state-actions	None
$p(\theta)$	Contextual Prior	Characterizes uncertainty in θ a priori at test time	\mathcal{D}_{Sim} - samples from the CMDP simulator
$p(a s, \theta, \omega)$	Model Expert Policy	Model of optimal policy for expert in CMDP $\mathcal{M}(\theta)$ with reward parameters ω	Contextual successor features learned from simulator and $\mathcal{D}_{\text{Expert}}$
$p(\omega \mathcal{D}_{\text{Expert}})$	Expert reward Posterior	Updates the reward parameter prior using expert data	$\mathcal{D}_{\text{Expert}}$ dataset of expert trajectories
$p(\theta_i \tau_i)$	Contextual Posterior	Characterizes uncertainty over which latent variable θ_i agent i was assigned	τ_i - each expert or exploratory agent's trajectory
$P_{\text{Bayes}}^{\text{IRL+COE}}(r s, a)$	Bayesian Reward Distribution	Incorporates epistemic uncertainty from $p(\omega \mathcal{D}_{\text{Expert}})$ and $p(k)$ into reward model	None

B Bayesian Successor Feature Learning

Consider the optimal Q -function $Q^*(s, a, \theta, \omega)$, which satisfies the optimal contextual Bellman equation: $\mathcal{B}^*[Q^*](s, a, \theta, \omega) = Q^*(s, a, \theta, \omega)$ where:

$$\begin{aligned} \mathcal{B}^*[Q^*](s, a, \theta, \omega) := & \nu(s, a)^\top \omega \\ & + \gamma \mathbb{E}_{s' \sim p(s'|s, a, \theta)} \left[\sup_{a'} Q^*(s', a', \theta, \omega) \right]. \end{aligned}$$

As the expert selects actions $a \in \arg \max_{a'} Q^*(s, a', \theta, \omega)$, learning $Q^*(s, a, \theta, \omega)$ is sufficient for modeling the set of expert policies, from which the true reward parametrization can be inferred.

Learning with Expert Data. Consider the Bellman equation under the expert policy $\pi^*(a'|s', \theta_i)$. The successor feature representation Ψ_ϕ should satisfy:

$$\Psi_\phi(s, a, \theta_i)^\top \omega^* = \nu(s, a)^\top \omega^* + \gamma \mathbb{E}_{s' \sim p(s'|s, a, \theta_i), a' \sim \pi^*(a'|s', \theta_i)} [\Psi_\phi(s', a', \theta_i)]^\top \omega^*.$$

We can factor ω^* from the Bellman equation and then solve:

$$\Psi_\phi(s, a, \theta_i) = \nu(s, a) + \gamma \mathbb{E}_{s' \sim p(s'|s, a, \theta_i), a' \sim \pi^*(a'|s', \theta_i)} [\Psi_\phi(s', a', \theta_i)].$$

This yields the objective for each expert trajectory τ_i :

$$\begin{aligned} \mathcal{L}_{\text{Expert}}(\phi; \tau_i) := & \mathbb{E}_{s, a \sim \text{Unif}(\tau_i), \theta_i \sim p(\theta_i|\tau_i)} [\|\Psi_\phi(s, a, \theta_i) - (\nu(s, a) \\ & + \gamma \mathbb{E}_{s' \sim p(s'|s, a, \theta_i), a' \sim \pi^*(a'|s', \theta_i)} [\Psi_\phi(s', a', \theta_i)])\|]. \end{aligned}$$

where $\text{Unif}(\tau_i)$ is a uniform distribution over the state-action pairs in trajectory τ_i . Minimizing $\mathcal{L}_{\text{Expert}}(\phi; \tau_i)$ for each trajectory ensures that the successor feature representation is consistent with the expert demonstrations. Minimizing $\mathcal{L}_{\text{Expert}}(\phi; \tau_i)$ can be carried out using a semi-gradient approach, thereby avoiding the need for two samples from the expert policy and state-transition distribution:

$$\phi \leftarrow \phi + \eta_\phi \nabla_\phi \Psi_\phi(s, a, \theta_i) (\nu(s, a) + \gamma \Psi_\phi(s', a', \theta_i) - \Psi_\phi(s, a, \theta_i)).$$

As the latent contextual variable θ_i is never observed, we must infer a posterior over its value $p(\theta_i|\tau_i)$. It may seem that this could be avoided via IRL using the prior-averaged transitions $\mathbb{E}_{\theta \sim p(\theta)} [p(s'|s, a, \phi)]$. However, we provide a simple counterexample in Appendix C demonstrating that a prior-averaged approach does not account for the true reward ordering in the underlying space of CMDPs. Sampling $\theta_i \sim p(\theta_i|\tau_i)$ from the posterior over the expert’s contextual variable is typically intractable, so we use variational inference instead, as detailed in Appendix E.

Learning with a Simulator. In addition to expert demonstrations, we also have access to samples from the CMDP simulator. This allows us to learn Ψ_ϕ over state-action pairs where the expert has not provided demonstrations. We sample a dataset $\mathcal{D}_{\text{Simulator}} := \{\tau_i\}_{i=1}^{N_{\text{Simulator}}}$ of $N_{\text{Simulator}}$ trajectories from the simulator: the simulator samples an MDP from the prior, and then an exploration policy π_{Explore} interacts with the corresponding MDP, observing state-action-state transitions. In this paper, we use an ϵ -greedy exploration policy where the greedy actions $a' \in \arg \max_{a'} \Psi_\phi(s', a', \theta_i)^\top \omega$ are taken with probability $1 - \epsilon$ then uniformly otherwise. More sophisticated approaches such as a policy that maximizes the entropy of the ergodic, discounted state-action occupancy distribution [14] would also be appropriate, especially in larger domains. However, our experiments demonstrate the ϵ -greedy policy suffices for learning successor features in our setting.

Once samples have been obtained, we infer the posterior $p(\theta_i|\tau_i)$ over the MDP that the exploratory agent was assigned for each MDP $i \in [1 : N_{\text{Simulator}}]$. Like with the expert data, our goal is to ensure that the successor feature representation Ψ_ϕ satisfies a Bellman equation. In the target, we choose the next action that maximizes the Q -function for a given ω , $a' \in \arg \max_{a'} \Psi_\phi(s', a', \theta_i)^\top \omega$. This yields the objective for each MDP i :

$$\mathcal{L}_{\text{Simulator}}(\phi; \tau_i, \omega) := \mathbb{E}_{s, a \sim \text{Unif}(\tau_i), \theta_i \sim p(\theta_i|\tau_i)} \left[\left(\Psi_\phi(s, a, \theta_i) - (\nu(s, a) + \gamma \mathbb{E}_{s' \sim p(s'|s, a, \theta_i)} [\Psi_\phi(s', a', \theta_i)]) \right)^2 \right].$$

where $\text{Unif}(\tau_i)$ is a uniform distribution over the state-action pairs in trajectory τ_i . We optimize this objective using the following TD update:

$$\phi \leftarrow \phi + \eta_\phi \nabla_\phi \Psi_\phi(s, a, \theta_i) \cdot (\nu(s, a) + \gamma \Psi_{\phi'}(s', a', \theta_i) - \Psi_\phi(s, a, \theta_i)).$$

There are two differences between the updates for the exploratory data and the expert data. First, the exploratory data updates are off-policy. Due to the deadly triad [29], using semi-gradients is not guaranteed to converge [11, 31]. We introduce a separate target network ϕ' that is updated periodically to stabilize the updates. Second, the updates depend on ω as the supremum acts over the dot product between the successor representation and the reward parametrization. As we require successor features to infer ω , we interleave learning both ω and ϕ in a nested optimization, using both expert and exploratory data with an initial burn-in period using only the expert data.

We combine both objectives into the single objective presented in Section 4.1:

$$\mathcal{L}(\phi; \omega) = \mathcal{L}_{\text{Expert}}(\phi; \tau_i) + \beta \mathcal{L}_{\text{Simulator}}(\phi; \tau_i, \omega),$$

for some constant β . However, we note that the reward learning and successor feature learning depend on each other through the objective $\mathcal{L}_{\text{Simulator}}$ and reward update given by Theorem 4.1, yielding a two-timescale learning problem. To enable convergence to a stable local optimum, the learning rates η_ϕ and η_ω are set such that $\eta_\omega < \eta_\phi$.

C The Need for Inference Over Context Variables

We consider a simple counterexample illustrated in Figure 6 with four states s_i and two possible hidden contexts denoted by θ . As shown in the figure, θ controls the environment transition. The simplest approach to IRL using the average MDP would map the experts’ state visitation frequency η to reward value. This would assign rewards: $r(s_1) = c\eta$, $r(s_2) = c(1 - \eta)$, $r(s_3) = c$, where c is an arbitrary finite positive constant. This means that the values of $r(s_1)$ and $r(s_2)$ are only determined by η and will give incorrect reward ordering $r(s_2) \geq r(s_1)$ for any $\eta \leq 0.5$. On the other hand, if a Bayesian approach is taken, it is possible to infer which MDP the agent was in. If the belief of a trajectory is weighted towards the expert being in $\theta = 0$, the expert’s preference for $a_0 = \text{left}$ over $a_1 = \text{right}$ must be a consequence of the reward ordering $r(s_1) > r(s_2)$. Likewise, if the belief of a trajectory is weighted towards the expert being in $\theta = 1$, the expert’s preference for $a_0 = \text{right}$ must imply that $r(s_2) + \gamma r(s_3) > r(s_1) + \gamma r(s_0)$. As $r(s_1) > r(s_2)$ will be inferred from the trajectories

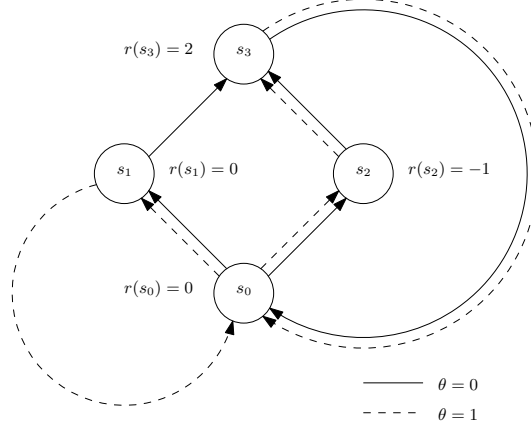


Figure 6: Counterexample CMDP

Algorithm 1 BAYESIAN SOLUTION TO THE IMITATION GAP

Require: priors $p(\theta)$, $p(\omega)$, and $p_{\text{COE}}(r|\sigma, s, a)$, contextual posterior $p(\theta|\tau)$, dataset $\mathcal{D}_{\text{Expert}}$, reward scales r_{\min} and r_{\max} , learning rates η_{ω} and η_{ϕ} , loss coefficient β , and number of steps K .

Initialize parameters ϕ for the successor features and ω for the reward.

Initialize an empty replay buffer $\mathcal{D}_{\text{Replay}}$.

for K steps **do**

 Sample a new MDP from simulator $\theta_i \sim \rho(\theta)$.

 Sample a trajectory τ_i in the MDP defined by θ_i using an epsilon-greedy policy w.r.t. the Q -function defined by $\Psi_{\phi}(s, a, \tilde{\theta}_i)^{\top} \omega$ for $\tilde{\theta}_i \sim p(\theta_i|\tau_i)$.

 Add the trajectory τ_i to the replay buffer $\mathcal{D}_{\text{Replay}}$.

 Update ϕ to minimise $\mathcal{L}(\phi; \omega)$ using $\mathcal{D}_{\text{Expert}}$ and $\mathcal{D}_{\text{Replay}}$.

 Update ω using Theorem 4.1 with $\mathcal{D}_{\text{Expert}}$.

end for

Rescale ω s.t. rewards lie in the range $[r_{\min}, r_{\max}]$.

Compute the predictive reward $r_{\text{Bayes}}^{\text{IRL} + \text{COE}}$.

return $r_{\text{Bayes}}^{\text{IRL} + \text{COE}}$

of experts in $\theta = 0$, this implies that $r(s_0) < r(s_3)$, and so a correct reward ordering will be learned regardless of η . By being Bayesian, these possible inferences condition on which θ_i the expert was in, and are explained by $Q_{\zeta^*}(s, a, \theta_i, \omega)$. We can best match ω so that is consistent with these inferences under the belief $p(\theta_i|\tau_i, \omega)$ in the expert's MDP. We thus conclude that compared to a fully Bayesian approach, naively using imitation learning on the prior-averaged MDP will not yield policies that account for reward ordering of the underlying MDP.

D Bayesian Solution to the Imitation Gap

Finally, we present pseudocode for the Bayesian solution to the Imitation Gap (BIG) in Algorithm 1. It takes as inputs the prior distributions and the expert dataset and produces a reward function $r_{\text{Bayes}}^{\text{IRL} + \text{COE}}$. In the main loop, data is collected from the simulated environment using an ϵ -greedy policy. We use ϵ -greedy for convenience as we found it to be an easy way to achieve suitable coverage of the state-action space in the experiments. The data collected using the random policy is used for learning the successor features in an off-policy RL algorithm. With an off-policy algorithm, assuming coverage of the whole state-action space, the exact kind of randomness does not matter for the kind of successor features we learn. The collected data together with the expert demonstrations are used to update the successor feature representation. The learned successor features are used for updating the reward parameters to maximize the likelihood of the expert data. After K steps of the main loop, the final reward function is computed by applying the cost-of-exploration refinement defined in Section 4.3.

E Approximate Inference

Whilst the full Bayesian approach outlined in Section 4 is clearly desirable, there are several sources of intractability that prevent us from computing the Bayes-optimal policy π_{Bayes}^* exactly. Firstly, maintaining and inferring the posterior distributions is likely to be intractable for all but the simplest choice of likelihoods, which have insufficient capacity for representing the set of MDPs beyond contrived toy tasks. Secondly, marginalization using the posteriors likely will involve high dimensional integrals, which are computationally inefficient. Finally, solving the planning problem in the BAMDP for every possible history to obtain a Bayes-optimal policy is notoriously challenging, even for very simple domains [37, 38]. We thus derive an algorithm that follows the methodology of the formal Bayesian approach outlined in Section 4 whilst making necessary approximations from the powerful toolkit of variational inference to ensure tractability.

E.1 Tractable Prior and Likelihood Learning

Instead of attempting to infer the posterior $p(\phi|\mathcal{D}_{\text{simulator}})$ exactly, which may be intractable, we use a MAP approach instead to learn a point estimate ϕ_{MAP}^* . The justification for this is that we have access to a simulator from which a large number of samples can be drawn. The Bernstein-von Mises theorem specifies that in the limit of large data $K \rightarrow \infty$, $p(\phi|\mathcal{D}_{\text{simulator}}) \rightarrow \delta_{\phi_{\text{MLE}}^*}(\phi)$ where ϕ_{MLE}^* is the maximum likelihood estimator, so we expect $p(\phi|\mathcal{D}_{\text{simulator}}) \approx \delta_{\phi_{\text{MLE}}^*}(\phi)$. In the same limit, $\phi_{\text{MAP}}^* \rightarrow \phi_{\text{MLE}}^*$. Our choice of using a MAP estimator over the MLE estimator is purely practical in that the prior can add regularization to stabilize learning, as is seen by the contribution to the MAP objective:

$$\mathcal{L}_{\text{MAP}}(\phi) = \sum_{i=1}^K \log p(\tau_i|\phi) + \log(\phi).$$

To find a tractable objective to maximize the MAP estimate, we introduce a variational distribution $q_{\chi_i}(\theta_i)$ parametrized by $\chi_i \in X$, for which:

$$\begin{aligned} \log p(\tau_i|\phi) &= \int \log p(\tau_i|\phi) q_{\chi_i}(\theta_i) d\theta_i, \\ &= \int \log \left(\frac{p(\tau_i, \theta_i|\phi)}{p(\theta_i|\tau_i, \phi)} \right) q_{\chi_i}(\theta_i) d\theta_i, \\ &= \int \log \left(\frac{p(\tau_i, \theta_i|\phi)}{p(\theta_i|\tau_i, \phi)} \cdot \frac{q_{\chi_i}(\theta_i)}{q_{\chi_i}(\theta_i)} \right) q_{\chi_i}(\theta_i) d\theta_i, \\ &= \int (\log p(\tau_i, \theta_i|\phi) - \log q_{\chi_i}(\theta_i)) q_{\chi_i}(\theta_i) d\theta_i - \int \frac{\log p(\theta_i|\tau_i, \phi)}{\log q_{\chi_i}(\theta_i)} q_{\chi_i}(\theta_i) d\theta_i, \end{aligned}$$

$$= \mathcal{L}_{\text{ELBO}}(\phi, \chi_i) + \text{KL}(q_{\chi_i} \parallel p(\cdot|\tau_i, \phi)),$$

$$\implies \mathcal{L}_{\text{ELBO}}(\phi, \chi_i) = \log p(\tau_i|\phi) - \text{KL}(q_{\chi_i} \parallel p(\cdot|\tau_i, \phi)),$$

where $\mathcal{L}_{\text{ELBO}}(\cdot)$ denotes an evidence lower bound (ELBO). Now, assuming there exists some $\chi_i^* \in X$ such that $q_{\chi_i^*}(\theta_i) = p(\theta_i|\tau_i, \phi)$, then $\sup_{\chi_i \in X} \text{KL}(q_{\chi_i} \parallel p(\cdot|\tau_i, \phi)) = 0$, hence it follows from Appendix E.1 that

$$\log p(\tau_i|\phi) = \sup_{\chi_i \in X} \mathcal{L}_{\text{ELBO}}(\phi, \chi_i).$$

Substituting into the MAP objective from Appendix E.1 yields:

$$\mathcal{L}_{\text{MAP}}(\phi) = \sum_{i=1}^K \sup_{\chi_i \in X} \mathcal{L}_{\text{ELBO}}(\phi, \chi_i) + \log(\phi).$$

To find a $\phi_{\text{MAP}}^* \in \arg \sup_{\phi \in \Phi} \mathcal{L}_{\text{MAP}}(\phi)$, we recognize that for each MDP sampled from the simulator indexed by $i \in [1 : K]$, we can minimize the following index-specific ELBO:

$$\mathcal{L}_{\text{ELBO}}(\phi, \chi_i) = \mathbb{E}_{\theta_i \sim q_{\chi_i}(\theta_i)} \left[\sum_{t=1}^{H_i} \log p(s_t|s_{t-1}, a_{t-1}, \theta_i) + \log p(\theta_i|\phi) - \log(q_{\chi_i}(\theta_i)) \right],$$

with respect to ϕ and χ_i . Here, Variational Auto-encoders [19] (VAEs) offer a powerful framework for solving this problem via a variational expectation-maximization (EM) algorithm. In VAE parlance, the distribution $p(\tau_i|\theta_i, \phi)$ is known as the *decoder*, parametrized by $\phi \in \Phi$.

Algorithm 2 LEARNPRIOR+LIKELIHOOD

```

Initialize  $\zeta, \chi, \phi$ 
for  $K$  steps do
  Sample new MDP from simulator  $\theta \sim \rho(\theta)$ 
  Sample initial state  $s_0 \sim p_0(s_0)$ 
  for  $t \in [1 : H_i]$  do
    Sample action  $a_{t-1} \sim d(a_{t-1})$ 
    Sample transition  $s_t \sim p(s_t|s_{t-1}, a_{t-1}, \theta)$ 
    Sample gradient  $g_\chi \sim \nabla_\psi \mathcal{L}_{\text{ELBO}}(\phi, \chi)$ 
     $\chi \leftarrow \chi + \alpha_\chi^t g_\chi$ 
    Sample gradient
     $g_\phi \sim \nabla_\phi \left( \mathcal{L}_{\text{ELBO}}(\phi, \chi) + \frac{1}{KH_i} \log p(\phi) \right)$ 
     $\phi \leftarrow \phi + \alpha_\phi^t g_\phi$ 
     $g_\zeta \sim \nabla_\zeta \text{MSBE}(\zeta)$ 
     $\zeta \leftarrow \zeta - \alpha_\zeta^t g_\zeta$ 
  end for
end for
return  $\zeta, \phi$ 

```

For each MDP θ_i , we train an *encoder* $q_{\chi_i}(\theta_i)$, parametrized by $\chi_i \in X$, that acts as a variational approximation to the posterior: $p(\theta_i|\tau_i, \phi)$.

To learn the prior parameters, we propose Algorithm 2. Instead of specifying an encoder for each $q_{\chi_i}(\theta_i)$, we train a single encoder $q_\chi(\theta_i)$ online using an entire trajectory of samples from a specific MDP θ_i . Once training has finished for that MDP, we sample another θ_{i+1} , using χ as the initialization parameters for the new encoder, $q_\chi(\theta_{i+1})$. Moreover, as both learning the reward prior and minimizing the MSBE to learn the likelihood require samples from a simulator, we interleave both optimization problems using the same interactions with the simulator.

F Proofs and Derivations

Lemma 4.1. *The gradient of the log normalization constant $\log z(s, \omega, \theta_i)$ is*

$$\nabla_\omega \log z(s, \omega, \theta_i) = \mathbb{E}_{a \sim p(a|s, \omega, \theta_i)} [\Psi^*(s, a, \theta_i)].$$

Proof. We assume that \mathcal{A} is continuous. If \mathcal{A} is discrete, we replace the Lebesgue measure λ with the counting measure, and our proof remains unchanged. Taking derivatives directly yields our desired result:

$$\begin{aligned}
\nabla_\omega \log z(s, \omega, \theta_i) &= \nabla_\omega \log \int_{\mathcal{A}} \exp\left(\frac{1}{\alpha} \Psi^*(s, a, \theta_i)^\top \omega\right) d\lambda(a), \\
&= \nabla_\omega \int_{\mathcal{A}} \exp\left(\frac{1}{\alpha} \Psi^*(s, a, \theta_i)^\top \omega\right) d\lambda(a) \cdot \frac{1}{\int_{\mathcal{A}} \exp\left(\frac{1}{\alpha} \Psi^*(s, a, \theta_i)^\top \omega\right) d\lambda(a)}, \\
&= \int_{\mathcal{A}} \Psi^*(s, a, \theta_i) \frac{\exp\left(\frac{1}{\alpha} \Psi^*(s, a, \theta_i)^\top \omega\right)}{\int_{\mathcal{A}} \exp\left(\frac{1}{\alpha} \Psi^*(s, a, \theta_i)^\top \omega\right) d\lambda(a)} d\lambda(a), \\
&= \int_{\mathcal{A}} \Psi^*(s, a, \theta_i) p(a|s, \omega, \theta_i) d\lambda(a), \\
&= \mathbb{E}_{a \sim p(a|s, \omega, \theta_i)} [\Psi^*(s, a, \theta_i)].
\end{aligned}$$

□

Theorem 4.1. Define $\varsigma_0^2 := \frac{\sigma_0^2}{\alpha}$. Using the Laplace approximation for the posterior, the approximate Bayesian reward parametrization $\omega_{\text{Bayes}}^* \approx \omega_{\text{Laplace}}^*$ can be found by carrying out the following stochastic gradient descent updates on the log-posterior:

$$\omega \leftarrow \omega + \eta_\omega \left(N_{\text{Expert}} H_i \left(\Psi^*(s_j, a_j, \theta_i) - \mathbb{E}_{a_i \sim p(a_i | s_j, \omega, \theta_i)} [\Psi^*(s_j, a_i, \theta_i)] \right) - \frac{(\omega - \omega_0)}{\varsigma_0^2} \right).$$

Proof. Using Laplace's approximation, we fit a Gaussian to the posterior distribution with mean $\omega_{\text{Laplace}}^* \in \arg \sup_{\omega \in \Omega} p(\omega | \mathcal{D}_{\text{Expert}})$. Equivalently, we can maximize the log posterior instead. Defining $g(\omega; \mathcal{D}_{\text{Expert}}) := \nabla_\omega \log p(\omega | \mathcal{D}_{\text{Expert}})$, from the definition of the gradient of a log:

$$g(\omega; \mathcal{D}_{\text{Expert}}) = \nabla_\omega \log p(\omega | \mathcal{D}_{\text{Expert}}) = \nabla_\omega p(\omega | \mathcal{D}_{\text{Expert}}) \cdot \frac{1}{p(\omega | \mathcal{D}_{\text{Expert}})}.$$

We define the joint set of expert contextual variables as $\Theta_{\text{Expert}} := \{\theta_1, \theta_2, \dots, \theta_{N_{\text{Expert}}}\} \in \Theta^{N_{\text{Expert}}}$. Taking gradients of the posterior yields:

$$\begin{aligned} \nabla_\omega p(\omega | \mathcal{D}_{\text{Expert}}) &= \int_{\Theta^{N_{\text{Expert}}}} \nabla_\omega p(\omega | \mathcal{D}_{\text{Expert}}, \Theta_{\text{Expert}}) dP(\Theta_{\text{Expert}} | \mathcal{D}_{\text{Expert}}), \\ &= \int_{\Theta^{N_{\text{Expert}}}} \frac{\nabla_\omega p(\omega | \mathcal{D}_{\text{Expert}}, \Theta_{\text{Expert}})}{p(\omega | \mathcal{D}_{\text{Expert}}, \Theta_{\text{Expert}})} p(\omega | \mathcal{D}_{\text{Expert}}, \Theta_{\text{Expert}}) dP(\Theta_{\text{Expert}} | \mathcal{D}_{\text{Expert}}), \\ &= \int_{\Theta^{N_{\text{Expert}}}} \nabla_\omega \log p(\omega | \mathcal{D}_{\text{Expert}}, \Theta_{\text{Expert}}) dP(\Theta_{\text{Expert}}, \omega | \mathcal{D}_{\text{Expert}}), \\ &= \int_{\Theta^{N_{\text{Expert}}}} \nabla_\omega \log p(\omega | \mathcal{D}_{\text{Expert}}, \Theta_{\text{Expert}}) dP(\Theta_{\text{Expert}} | \omega, \mathcal{D}_{\text{Expert}}) p(\omega | \mathcal{D}_{\text{Expert}}). \end{aligned}$$

Substituting yields our desired result:

$$\nabla_\omega \log p(\omega | \mathcal{D}_{\text{Expert}}) = \int_{\Theta^{N_{\text{Expert}}}} \nabla_\omega \log p(\omega | \mathcal{D}_{\text{Expert}}, \Theta_{\text{Expert}}) dP(\Theta_{\text{Expert}} | \omega, \mathcal{D}_{\text{Expert}}).$$

Now,

$$\begin{aligned} p(\omega | \mathcal{D}_{\text{Expert}}, \Theta_{\text{Expert}}) &= \frac{p(\mathcal{D}_{\text{Expert}} | \omega, \Theta_{\text{Expert}}) p(\omega)}{\int p(\mathcal{D}_{\text{Expert}} | \omega, \Theta_{\text{Expert}}) dP(\omega)}, \\ &= \frac{\prod_{i=1}^{N_{\text{Expert}}} p(\tau_i | \omega, \theta_i) p(\omega)}{\int \prod_{i=1}^{N_{\text{Expert}}} p(\tau_i | \omega, \theta_i) dP(\omega)}, \\ &= \frac{\prod_{i=1}^{N_{\text{Expert}}} \prod_{j=0}^{H_i-1} p(s_{j+1} | s_j, a_j, \theta_i) p(a_j | s_j, \omega, \theta_i) p(\omega)}{\int \prod_{i=1}^{N_{\text{Expert}}} \prod_{j=0}^{H_i-1} p(s_{j+1} | s_j, a_j, \theta_i) p(a_j | s_j, \omega, \theta_i) dP(\omega)}, \\ &= \frac{\prod_{i=1}^{N_{\text{Expert}}} \prod_{j=0}^{H_i-1} p(a_j | s_j, \omega, \theta_i) p(\omega)}{\int \prod_{i=1}^{N_{\text{Expert}}} \prod_{j=0}^{H_i-1} p(a_j | s_j, \omega, \theta_i) dP(\omega)}, \end{aligned}$$

where we have used the fact that each $p(s_{j+1} | s_j, a_j, \theta_i)$ has no dependence on ω , and so will cancel in the fraction when deriving the final line. Now, substituting for the definition of the likelihood:

$$\begin{aligned} &p(\omega | \mathcal{D}_{\text{Expert}}, \Theta_{\text{Expert}}) \\ &\propto \underbrace{\exp \left(\sum_{i=1}^{N_{\text{Expert}}} \sum_{j=0}^{H_i-1} \left(\frac{\Psi^*(s_j, a_j, \theta_i)^\top \omega}{\alpha} - \log z(s_j, \theta_i, \omega) \right) \right)}_{\text{Likelihood}} \underbrace{\exp \left(-\frac{\|\omega - \omega_0\|^2}{2\sigma_0^2} \right)}_{\text{Prior}}, \\ &= \exp \left(\sum_{i=1}^{N_{\text{Expert}}} \sum_{j=0}^{H_i-1} \left(\frac{\Psi^*(s_j, a_j, \theta_i)^\top \omega}{\alpha} - \log z(s_j, \theta_i, \omega) \right) - \frac{\|\omega - \omega_0\|^2}{2\sigma_0^2} \right), \end{aligned}$$

hence:

$$\begin{aligned}
& \nabla_{\omega} \log p(\omega | \mathcal{D}_{\text{Expert}}, \Theta_{\text{Expert}}) \\
&= \nabla_{\omega} \left(\sum_{i=1}^{N_{\text{Expert}}} \sum_{j=0}^{H_i-1} \left(\frac{\Psi^*(s_j, a_j, \theta_i)^\top \omega}{\alpha} - \log z(s_j, \theta_i, \omega) \right) - \frac{\|\omega - \omega_0\|^2}{2\sigma_0^2} \right), \\
&\implies g(\omega; \mathcal{D}_{\text{Expert}}) \\
&= \int_{\Theta^{N_{\text{Expert}}}} \nabla_{\omega} \left(\sum_{i=1}^{N_{\text{Expert}}} \sum_{j=0}^{H_i-1} \left(\frac{\Psi^*(s_j, a_j, \theta_i)^\top \omega}{\alpha} - \log z(s_j, \theta_i, \omega) \right) \right. \\
&\quad \left. - \frac{\|\omega - \omega_0\|^2}{2\sigma_0^2} \right) dP(\Theta_{\text{Expert}} | \omega, \mathcal{D}_{\text{Expert}}), \\
&= \sum_{i=1}^{N_{\text{Expert}}} \mathbb{E}_{\theta_i \sim p(\theta_i | \omega, \tau_i)} \left[\nabla_{\omega} \left(\sum_{j=0}^{H_i-1} \left(\frac{\Psi^*(s_j, a_j, \theta_i)^\top \omega}{\alpha} - \log z(s_j, \theta_i, \omega) \right) - \frac{\|\omega - \omega_0\|^2}{2\sigma_0^2} \right) \right].
\end{aligned}$$

Now, applying Lemma 4.1 and multiplying by α yields:

$$\begin{aligned}
\alpha g(\omega; \mathcal{D}_{\text{Expert}}) &= \sum_{i=1}^{N_{\text{Expert}}} \sum_{j=0}^{H_i-1} \mathbb{E}_{\theta_i \sim p(\theta_i | \omega, \mathcal{D}_{\text{Expert}})} \left[(\Psi^*(s_j, a_j, \theta_i) - \mathbb{E}_{a_i \sim p(a_i | s_j, \omega, \theta_i)} [\Psi^*(s_j, a_i, \theta_i)]) \right] \\
&\quad - \frac{(\omega - \omega_0)}{\varsigma_0^2},
\end{aligned}$$

as required □

F.1 Derivation of BRL Objective

Starting from the Bayesian RL objective:

$$\begin{aligned}
J_{\text{Bayes}}^{\pi} &= \mathbb{E}_{\tau_{\infty} \sim p_{\infty}^{\pi}(\tau_{\infty})} \left[\sum_{i=0}^{\infty} \gamma^i r_i \right], \\
&= \mathbb{E}_{h_{\infty} \sim p_{\infty}^{\pi}(h_{\infty})} \left[\sum_{i=0}^{\infty} \gamma^i \mathbb{E}_{r_i \sim p(r_i | h_i, a_i)} [r_i] \right].
\end{aligned}$$

Now,

$$\begin{aligned}
\mathbb{E}_{r_i \sim p(r_i | h_i, a_i)} [r_i] &= \mathbb{E}_{r_i \sim p_{\text{Bayes}}^{\text{IRL+COE}}(r_i | s_i, a_i)} [r_i], \\
&= \begin{cases} \mathbb{E}_{k \sim p(k)} [\mathbb{E}_{r_i \sim p(r_i | s_i, a_i, k)} [r_i]], & s, a \in \mathcal{S}_{\text{COE}} \times \mathcal{A}_{\text{COE}}, \\ \mathbb{E}_{\omega \sim p(\omega)} [\mathbb{E}_{r_i \sim p(r_i | s_i, a_i, \omega)} [r_i]], & \text{otherwise,} \end{cases} \\
&= \begin{cases} \mathbb{E}_{k \sim p(k)} [kr_{\max}], & s, a \in \mathcal{S}_{\text{COE}} \times \mathcal{A}_{\text{COE}}, \\ \mathbb{E}_{\omega \sim p(\omega)} [\nu(s_i, a_i)^\top \omega], & \text{otherwise,} \end{cases} \\
&= \begin{cases} k^* r_{\max}, & s, a \in \mathcal{S}_{\text{COE}} \times \mathcal{A}_{\text{COE}}, \\ \nu(s_i, a_i)^\top \omega_{\text{Bayes}}^*, & \text{otherwise,} \end{cases} \\
&= r_{\text{Bayes}}^{\text{IRL+COE}}(s_i, a_i),
\end{aligned}$$

hence:

$$\begin{aligned}
J_{\text{Bayes}}^{\pi} &= \mathbb{E}_{h_{\infty} \sim p_{\infty}^{\pi}(h_{\infty})} \left[\sum_{i=0}^{\infty} \gamma^i r_{\text{Bayes}}^{\text{IRL+COE}}(s_i, a_i) \right], \\
&= \mathbb{E}_{\theta_{\text{test}} \sim p(\theta_{\text{test}})} \left[\mathbb{E}_{h_{\infty} \sim p_{\infty}^{\pi}(h_{\infty} | \theta)} \left[\sum_{i=0}^{\infty} \gamma^i r_{\text{Bayes}}^{\text{IRL+COE}}(s_i, a_i) \right] \right],
\end{aligned}$$

as required.

G The Role of Temperature in IRL

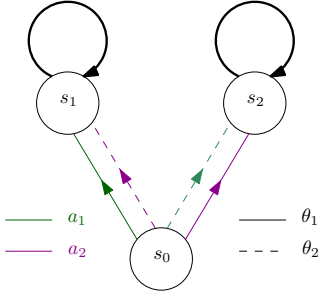


Figure 7: Space of Three State MDPs

We now provide an intuitive example to demonstrate how the prior influences the expert data in our Bayesian formulation. Consider the space of three state MDPs in Figure 7. The agent has a set of two possible actions $\mathcal{A} = \{a_1, a_2\}$. For $\theta = \theta_1$, the agent transitions to state s_1 deterministically after selecting a_1 or s_2 after selecting a_2 . For $\theta = \theta_2$, the actions are reversed. In both MDPs, the initial state is s_0 and state s_1 or s_2 are terminal. The reward function depends only on states and is $r(s_0) = 0, r(s_1) = 1, r(s_2) = -1$. Let $\mathbb{I}(s) \in \{0, 1\}^3$ denote the indicator feature vector where $I(s_n)$ is a one-hot vector where the n th element is 1, e.g. $\mathbb{I}(s_1) = (0, 1, 0)^\top$. We represent this reward function using the linear form $r(s) = \mathbb{I}(s)^\top \omega^*$ where $\omega^* = (0, 1, -1)^\top$. Finally, MDPs are allocated using a uniform prior.

Expert data will always consist of trajectories that transition from state s_0 to state s_1 . For our feature vector, we can derive the corresponding expert successor feature representation analytically:

$$\begin{aligned} \Psi^*(s_0, a_1, \theta_1) &= \mathbb{I}(s_0) + \frac{\gamma}{1-\gamma} \mathbb{I}(s_1), & \Psi^*(s_0, a_2, \theta_1) &= \mathbb{I}(s_0) + \frac{\gamma}{1-\gamma} \mathbb{I}(s_2), \\ \Psi^*(s_0, a_2, \theta_2) &= \mathbb{I}(s_0) + \frac{\gamma}{1-\gamma} \mathbb{I}(s_1), & \Psi^*(s_0, a_1, \theta_2) &= \mathbb{I}(s_0) + \frac{\gamma}{1-\gamma} \mathbb{I}(s_2), \\ \Psi^*(s_1, \cdot, \cdot) &= \frac{1}{1-\gamma} \mathbb{I}(s_1), & \Psi^*(s_2, \cdot, \cdot) &= \frac{1}{1-\gamma} \mathbb{I}(s_2). \end{aligned}$$

Using the gradient update in Theorem 4.1, we see that updates in state s_0 will initially draw actions equally from $p(a_i | s_0, \omega, \cdot)$. This yields an initial gradient update of:

$$\begin{aligned} g_\omega^0 &= \omega_0 + \eta_\omega^0 \frac{N_{\text{Expert}} H_i}{2} \left(\Psi^*(s_0, a_1, \theta_1) - \frac{1}{2} [\Psi^*(s_0, a_1, \theta_1) + \Psi^*(s_0, a_2, \theta_1)] \right) + \\ &\quad \eta_\omega \frac{N_{\text{Expert}} H_i}{2} \left(\Psi^*(s_0, a_2, \theta_2) - \frac{1}{2} [\Psi^*(s_0, a_2, \theta_2) + \Psi^*(s_0, a_1, \theta_2)] \right), \\ &= \omega_0 + \frac{\gamma \eta_\omega^0 N_{\text{Expert}} H_i}{2(1-\gamma)} [\mathbb{I}(s_1) - \mathbb{I}(s_2)]. \end{aligned}$$

For exposition, assume that there is no prior preference between ω_0^1 and ω_0^2 , and that $\omega_0^1 = \omega_0^2 = 0$. We see that the initial gradient will update these values to:

$$\omega_1^1 = \frac{\gamma \eta_\omega^0 N_{\text{Expert}} H_i}{2(1-\gamma)}, \quad \omega_1^2 = -\frac{\gamma \eta_\omega^0 N_{\text{Expert}} H_i}{2(1-\gamma)}.$$

We now consider the regime where the temperature parameter tends to zero $\alpha \rightarrow 0$. For all future updates, as $\omega_1 > \omega_2$, the model expert policy will tend towards a deterministic function that picks the action leading to state s_1 : $p(a | s_0, \omega, \theta_i) = \delta(a = a_i)$. This means that all future updates $k \geq 1$ from state s_0 will pull the reward parametrization back to the prior value:

$$g_\omega^k = \omega_k - \frac{\eta_\omega^k (\omega_k - \omega_0)}{\zeta_0^2}.$$

In the regime where the temperature parameter tends to infinity $\alpha \rightarrow \infty$, the model expert policy will remain uniform over all actions. Under this assumption, all future updates $k \geq 1$ from state s_0 will continue to increase the value of ω_1 and decrease the value of ω_2 , whilst pulling ω_k back towards the prior in accordance with ζ_0^2 .

$$g_\omega^k = \omega_k + \frac{\gamma \eta_\omega^k N_{\text{Expert}} H_i}{2(1-\gamma)} [\mathbb{I}(s_1) - \mathbb{I}(s_2)] - \frac{\eta_\omega^k (\omega_k - \omega_0)}{\zeta_0^2}.$$

When used in practice, we select α to be between 0 and ∞ . Our example reveals that the smaller the temperature parameter, the less the updates will separate values of reward for states that the expert visited vs that the expert could have visited. Conversely, when α is very large, this difference will grow and can only be counteracted by the prior variance ζ_0 .

H Experiments

H.1 Computer resources

The experiments were run on servers with eight recent NVIDIA GPUs (3080, A4500, or A5000). The random seeds were run in parallel. The experiments for the gridworld were the longest and took approximately an hour to run.

H.2 Latent Inference Investigation Details

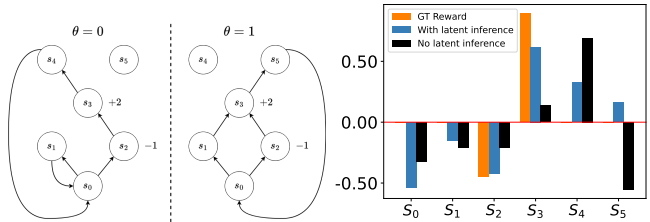


Figure 8: A demonstration of the necessity for latent inference. On the left, we repeat the visualization of the CMDP used in the experiments for convenience. On the right, we show the rewards learned with and without latent inference compared to the ground truth rewards. The reward vectors are normalized to unit norm. The y-axis is linearly scaled.

Figure 8 shows the learned rewards in the latent inference experiment described in Section 5.2. The learned rewards are somewhat hard to interpret because in addition to the scaling and shifting information being lost in IRL, there is no pressure for the algorithms to keep the reward vectors sparse. Instead, they are only trying to optimize Theorem 4.1. Nevertheless, the rewards learned with latent inference have the same ordering between the critical states s_1, s_2 , and s_3 as the ground truth reward. In contrast, the rewards learned with naive IRL do not differentiate between s_1 and s_2 , which results in the learned policies not taking the path through s_1 even when it is available.

H.3 Tiger Treasure Details

The Tiger-Treasure problem is displayed in Figure 1 and described in Section 3.1. The agent starts in state S_0 and can either listen or open a door. The listening action transitions the agent to a 'hint' state revealing with probability $p = 0.85$ the location of the Tiger. After the agent opens a door, it is either roared by the tiger or collects the treasure and arrives in the terminal state S_T . For learning the contextual IRL reward, we use the hyperparameters presented in Table 2 with a default value of $\omega_0 = (0, 0, 0, 0, 0)$ in the Laplace approximation Equation 4.1. The reward prior is introduced after having rescaled the IRL reward between $r_{\min} = -100$ and $r_{\max} = 10$. To enhance the training process, we normalize the rewards before training the DQN policies. The hyperparameters presented in Table 3.

Parameter	Value
Number of parallel environments	500
Number of steps per rollout	50
Number of updates	5000
ϵ -greedy ϵ	0.5
Maximum gradient norm	0.5
Discount γ	0.99
α	0.01
ζ_0^2	100.0
Target SF update rate	50
SF learning rate	1×10^{-3}
Reward learning rate	1×10^{-2}
Replay buffer size	50000
Batch size (trajectories)	500
r_{\max}	10.0
r_{\min}	-100.0

Table 2: IRL Hyperparameters for the Tiger Treasure problem.

Parameter	Value
Number of parallel environments	16
Number of steps per rollout	50
Total number of updates	20000
Learning rate	1×10^{-4}
Discount γ	0.99
Target network update rate	1
Replay buffer size (number of full trajectories)	200000
Batch size (number of full trajectories)	100
Starting value for ϵ	1.0
Final value for ϵ	0.05
Fraction of updates after ϵ schedule finishes	0.5

Table 3: DQN Hyperparameters for the Tiger Treasure problem.

H.4 Tiger Treasure Maze Details

The agent starts in the middle of the two doors. It can choose to move in the cardinal directions or listen. After the agent opens a door, it will either collect a treasure or be roared at by a tiger for one timestep. Then, depending on what happened, it gets transported to the nearest grid cell to the *Tiger* or *Gold*. The expert takes the shortest path to *Gold* and never listens. The state of the agent is defined as the $X - Y$ coordinates of the agent and an indicator variable, which indicates the result of the listening action. After taking a listening action, the agent is transported to a state with the same $X - Y$ coordinates but with the indicator showing the true value of θ . The indicator states have the same dynamics as the corresponding normal states. The coordinates and the indicator are encoded as one-hot vectors. The reward feature ν is the full table of all states visitable by the agent. Since the dynamics are deterministic given θ , the inference model labels the trajectories with the true θ if it is revealed on the trajectory.

The hyperparameters used for BIG in the maze experiment are shown in Table 4. The hyperparameters for DQN in the maze experiment are shown in Table 5. A recurrent neural network is used for the policy architecture. A separate MLP network is used for implementing the critic.

Parameter	Value
Number of parallel environments	16
Number of steps per rollout	40
Number of updates	20000
ϵ -greedy ϵ	0.5
Maximum gradient norm	0.5
Discount γ	0.99
α	0.01
ζ_0^2	1.0
Target SF update rate	50
SF learning rate	3×10^{-4}
Reward learning rate	3×10^{-3}
Replay buffer size (number of full trajectories)	10000
Batch size (number of full trajectories)	100
k	0.01
r_{\max}	1.0
r_{\min}	-0.05

Table 4: IRL Hyperparameters for the Maze problem.

Parameter	Value
Number of parallel environments	16
Number of steps per rollout	40
Total number of updates	100000
Learning rate	1×10^{-4}
Discount γ	0.99
Target network update rate	1
Replay buffer size (number of full trajectories)	10000
Batch size (number of full trajectories)	100
Starting value for ϵ	1.0
Final value for ϵ	0.05
Fraction of updates after ϵ schedule finishes	0.5

Table 5: DQN Hyperparameters for the Maze problem.